Microscopic theory of the neutron star crust

Seattle 2007

From the surface to the interior of a neutron star

1. Atmosphere. Atoms and molecules in a strong magnetic field.

2. Outer cust. Nuclei immersed in an electron gas.
   Essentially a solid state problem. Only nuclear data needed,
   except close to the drip point.

3. Inner crust. "Exotic nuclei" immersed in a neutron gas.
   Nuclear matter from very low density up to about saturation.
   Very asymmetric nuclear matter

4. "Pasta phase" of nuclear matter.

5. Interior. Homogeneous asymmetric nuclear matter above
   saturation

6. "Exotic matter" . Hyperons. Kaons? Pions? Quarks ?

Outer Crust

Inner Crust

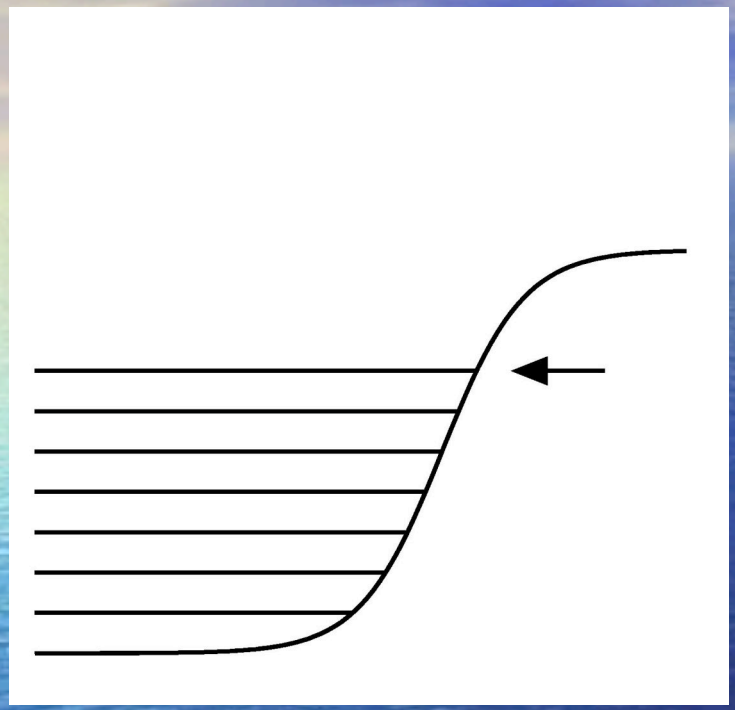

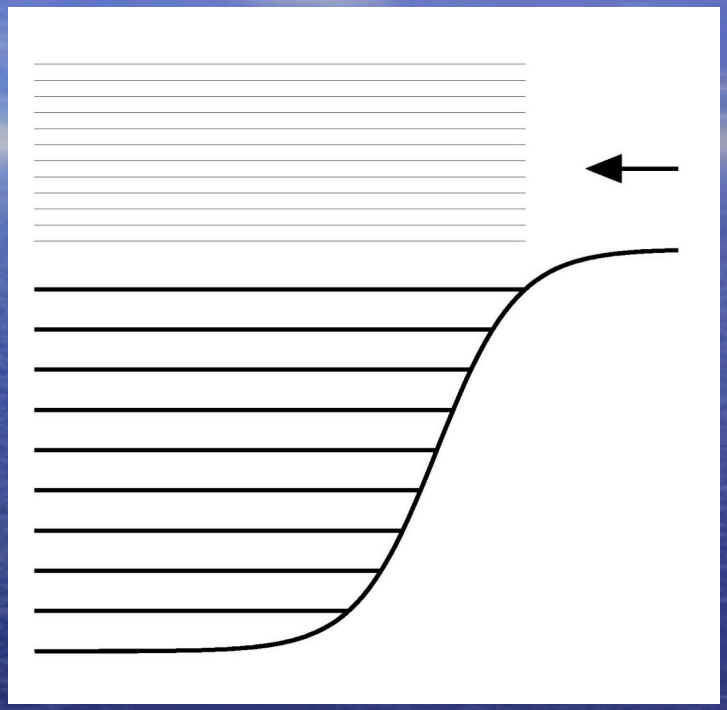

No drip

Drip region

Position of the neutron chemical potential

Drip point separates the inner crust from the outer one.

The outer crust is a crystal system consisting of nuclei immersed in a sea of ultra-relativistic electrons. At a critical density ρ_d (drip point) the neutron chemical potential μ_n vanishes.

ρ_d was found first by G.Baym, C.Pethick and P.Sutherland (BPS),1971, $\rho_d = 4.3 * 10^{11}\ \mathrm{g/cm^3}$

With extrapolation of the nuclear mass data. It was confirmed by NV, the last bound nucleus being ^{118}Kr (Z=36).

Recently : S.B.Ruster et al. , Phys.Rev. C73, 035804 (2006), carried out a systematic analysis of the outer crust in vicinity of ρ_d within the BPS method, with different models for EoS (Skyrme, droplet, relativistic NMF,…): $\rho_d \sim 4 \times 10^{11}$ g/cm^3, Z=34 –38.

EOS for the outer crust

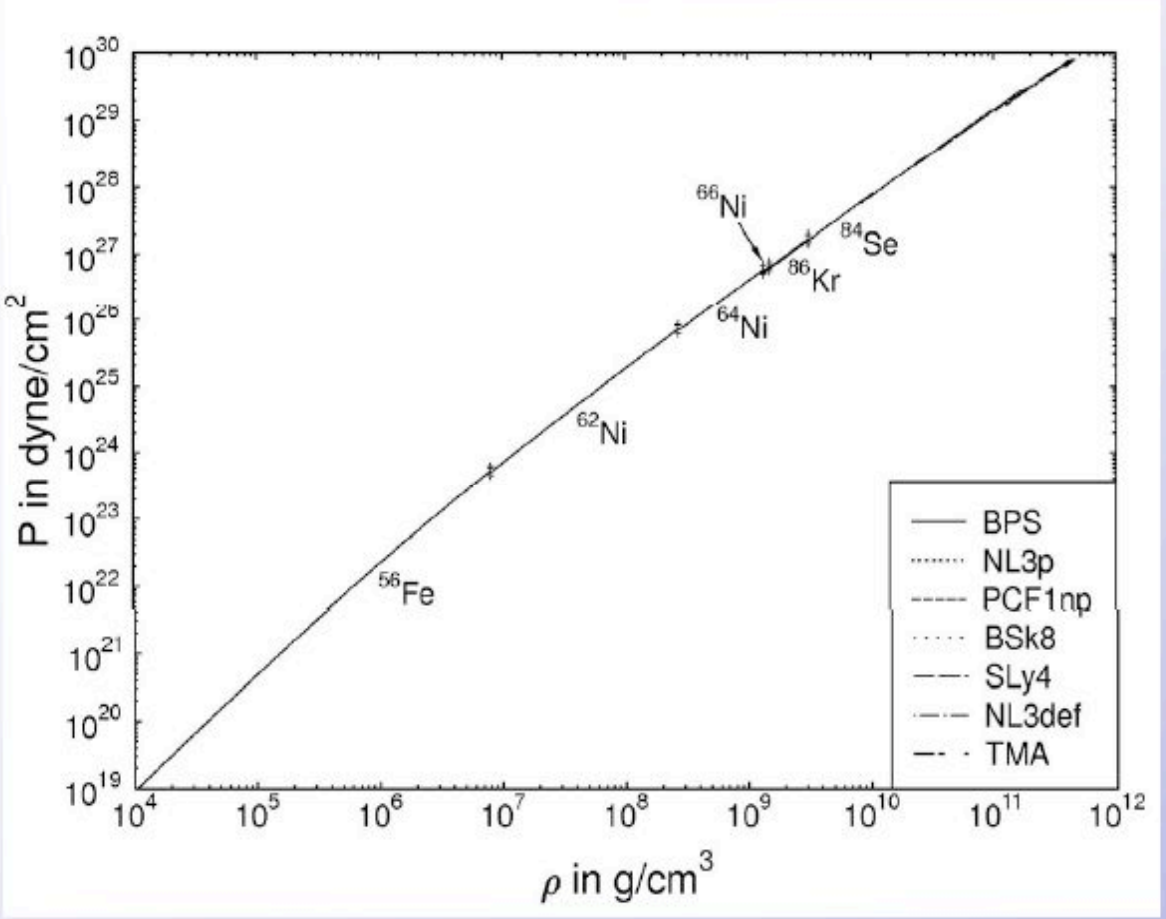

- up to $\rho \sim 10^{10}$ g/cm^3 sequences are identical (same experimental data)
- last common nuclei: ^{84}Se
- differences in BPS: ^{66}Ni and ^{86}Kr were not found
- but: EoS shows no noticeable differences, almost model-independent

S. Ruster, M. Hempel and J. Schaffner-Bielich, PRC 73, 035804 (2006)

Going close to the drip line

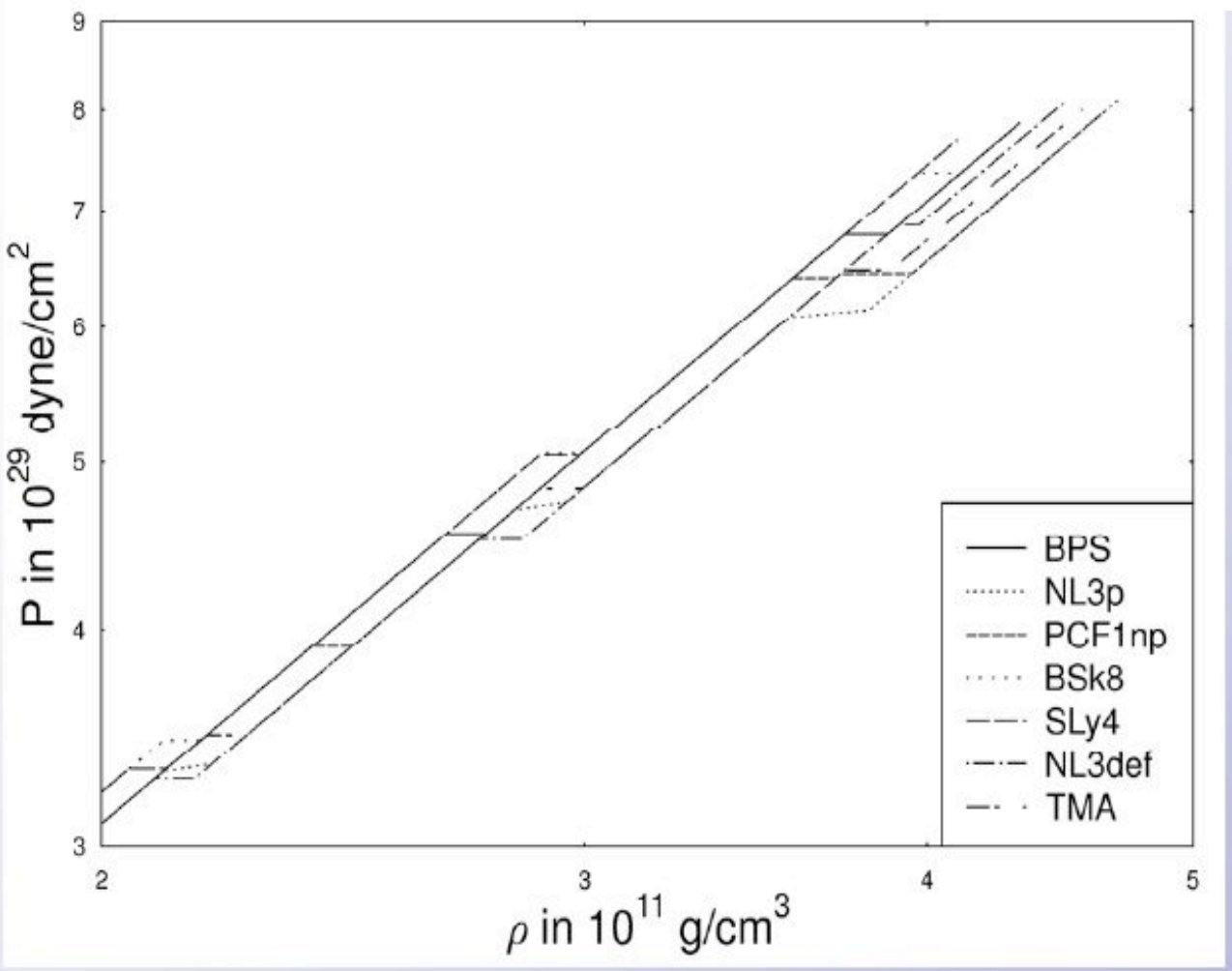

- models separate from each other at high mass density
- about 10% maximum deviation
- jumps in the mass density as predicted
- neutron drip around ρ=4-5¢10^{11}g/cm^3

Closer to the drip line "exotic" nuclei start to appear. This means that extrapolation to high asymmetry is needed.

The last non-dripping nucleus is expected to be 118 Kr

The method of energy density functional : mean field with effective interaction

A simple example

$$E[\hat{\rho}] = <\Phi|\hat{H}|\Phi> = \int d\vec{r}\mathcal{H}(\vec{r})$$

$$\mathcal{H}(\vec{r}) = \frac{\hbar^2}{2m}\tau(\vec{r}) + \frac{3t_0}{8}\rho^2(\vec{r}) + \frac{t_3}{16}\rho^3(\vec{r})$$

where

$$\tau(\vec{r}) = \frac{\hbar^2}{2M}\sum_i (\nabla\psi_i)^2$$

is the kinetic energy

In homogeneous matter

$$\tau(\vec{r}) = \frac{3}{5}\left(\frac{6\pi^2}{g}\right)^{2/3}\rho^{5/3}(\vec{r})$$

→ **EOS**

The parameters are adjusted to reproduce the empirical saturation point of symmetric nuclear matter.

In finite nuclei the minimization procedure gives the Hartree-Fock equations

↓

Binding energy, radii, nuclear structure

In general one can introduces a more complex structure for the effective forces (gradient terms, etc.) and correspondingly more parameters

$$\mathcal{H} = \mathcal{K} + \mathcal{H}_0 + \mathcal{H}_3 + \mathcal{H}_{eff} + \mathcal{H}_{fin} + \mathcal{H}_{so} + \mathcal{H}_{sg}$$

$$\begin{aligned}
\mathcal{K} &= \frac{\hbar^2}{2m}\tau \\
\mathcal{H}_0 &= \frac{t_0}{4}[(2+x_0)\rho^2 - (2x_0+1)(\rho_n^2+\rho_p^2)] \\
\mathcal{H}_3 &= \frac{t_3}{24}\rho^\sigma[(2+x_3)\rho^2 - (2x_3+1)(\rho_p^2+\rho_n^2)] \\
\mathcal{H}_{eff} &= \frac{1}{8}[t_1(2+x_1)+t_2(2+x_2)]\tau\rho + \frac{1}{8}[t_2(2x_2+1)-t_1(2x_1+1)](\tau_n\rho_n+\tau_p\rho_p) \\
\mathcal{H}_{fin} &= \frac{1}{32}[3t_1(2+x_1)-t_2(2+x_2)](\nabla\rho)^2 - \frac{1}{32}[3t_1(2x_1+1)+t_2(2x_2+1)]\left[(\nabla\rho_n)^2+(\nabla\rho_p)^2\right] \\
\mathcal{H}_{so} &= \frac{W_0}{2}[\vec{J}\cdot\nabla\rho + \vec{J}_p\cdot\nabla\rho_p + \vec{J}_n\cdot\nabla\rho_n] \\
\mathcal{H}_{sg} &= -\frac{1}{16}(t_1x_1+t_2x_2)\vec{J}^2 + \frac{1}{16}(t_1-t_2)\left[\vec{J}_n^2+\vec{J}_p^2\right]
\end{aligned}$$

In this case it is possible to reproduce not only the saturation point but also the binding energy and radii of spherical nuclei with a high degree of accuracy (better than 1% !) and many spectroscopic data (giant resonances, and so on)

However in the inner crust one needs to extrapolate the functionals to very high asymmetry, where they have not been tested. Furthermore the density dependence can be quite different

Spread in the symmetry energy even below saturation

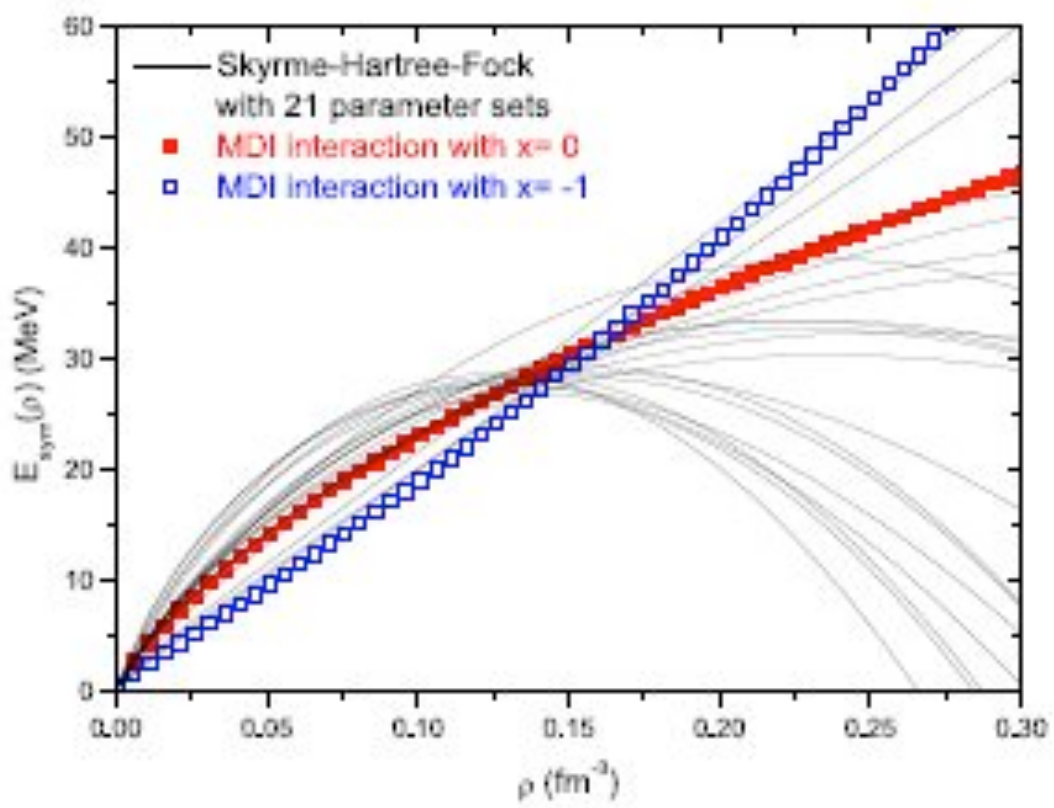

Bao-An Li et al., nucl-th/ 0610057

Spread in the neutron matter EOS

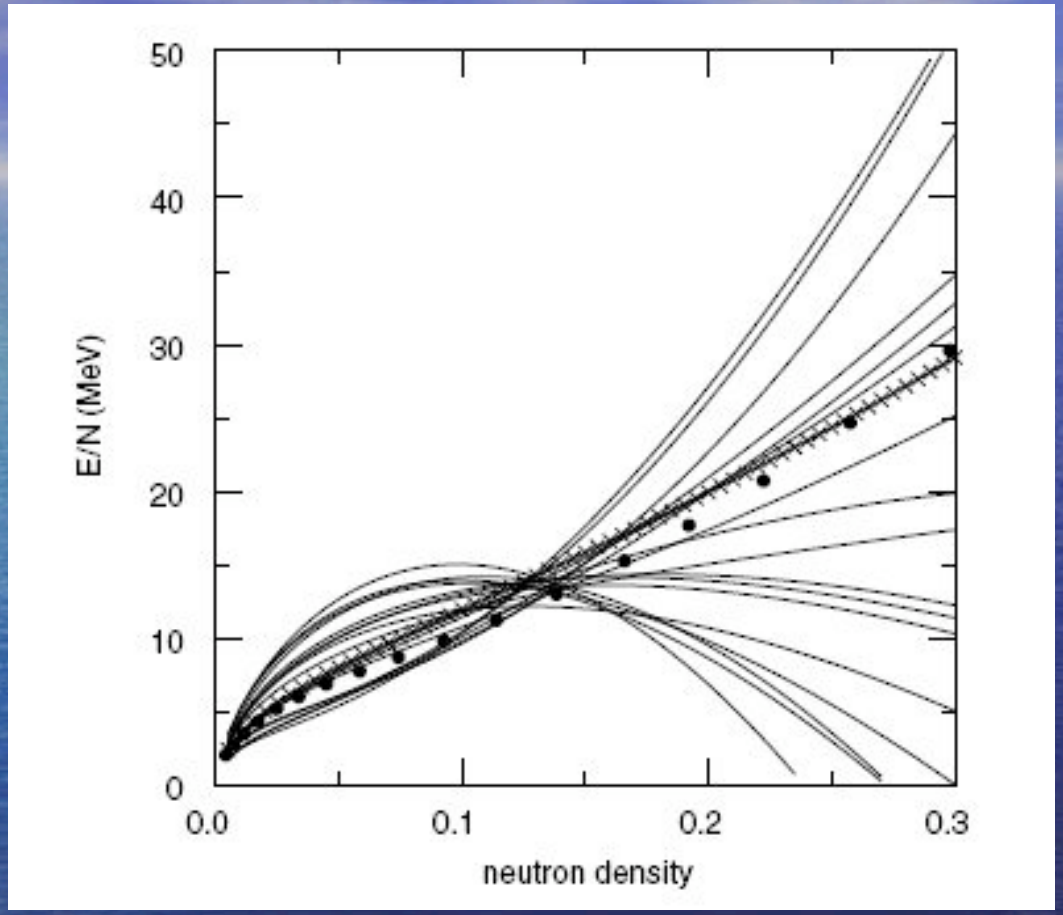

B. Alex Brown PRL 85 (2000) 5296

Symmetry energy, "low density"

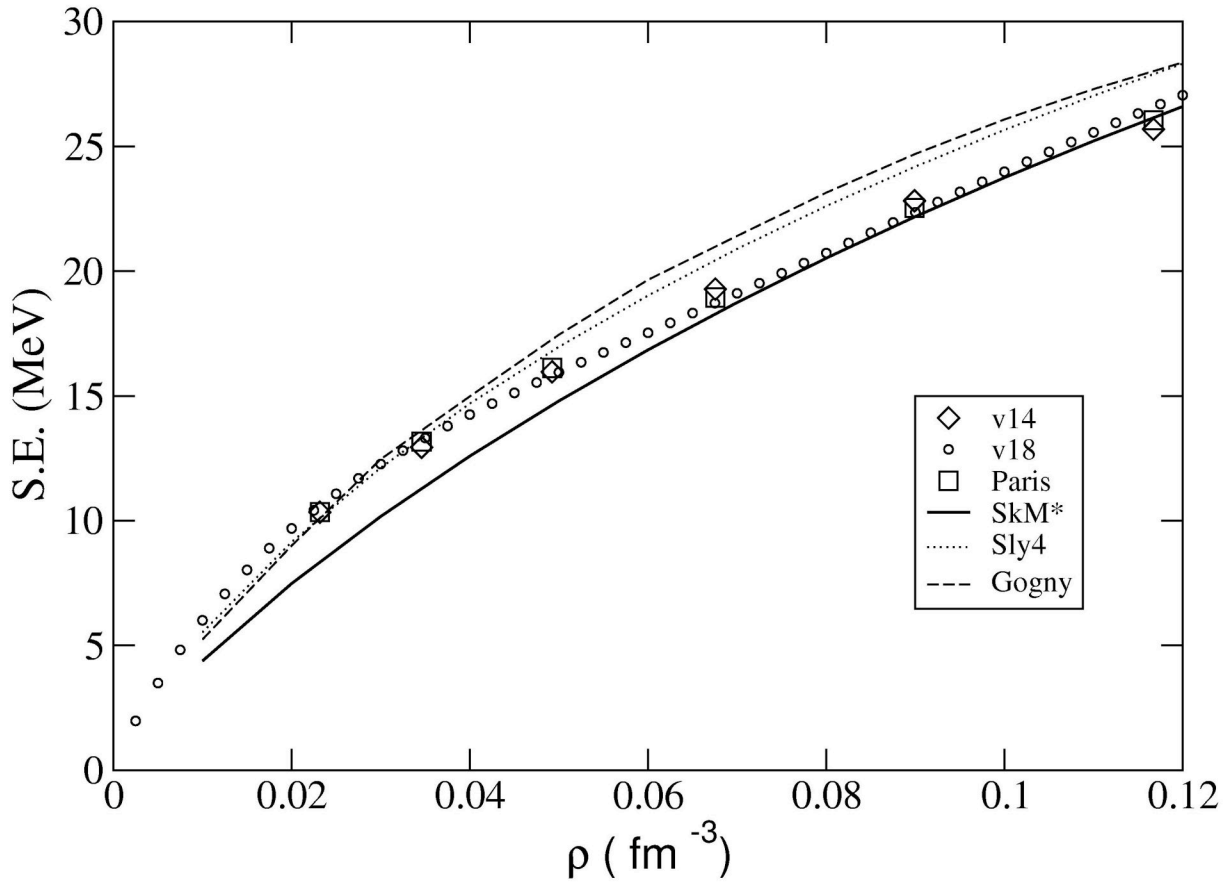

Symmetry energy as a function of density

Microscopic results approximately fitted by $31.3\,(\rho/\rho_0)^{0.6}$

M.Baldo, C. Maieron, P. Schuck and X. Vinas, Nucl. Phys. A **736**, 241 (2004).

Wigner – Seitz (WS) method

Crystal matter is approximated with a set of independent spherical cells of the radius R_C.

The cell contains Z protons, N=A-Z neutrons,

$$A = (4\pi / 3) R_c^3 \rho$$

And Z electrons (to be electroneutral).

β-stability condition:

$$\mu_n - (\mu_p + \mu_e) = 0.$$

Non-homogeneous nuclear matter

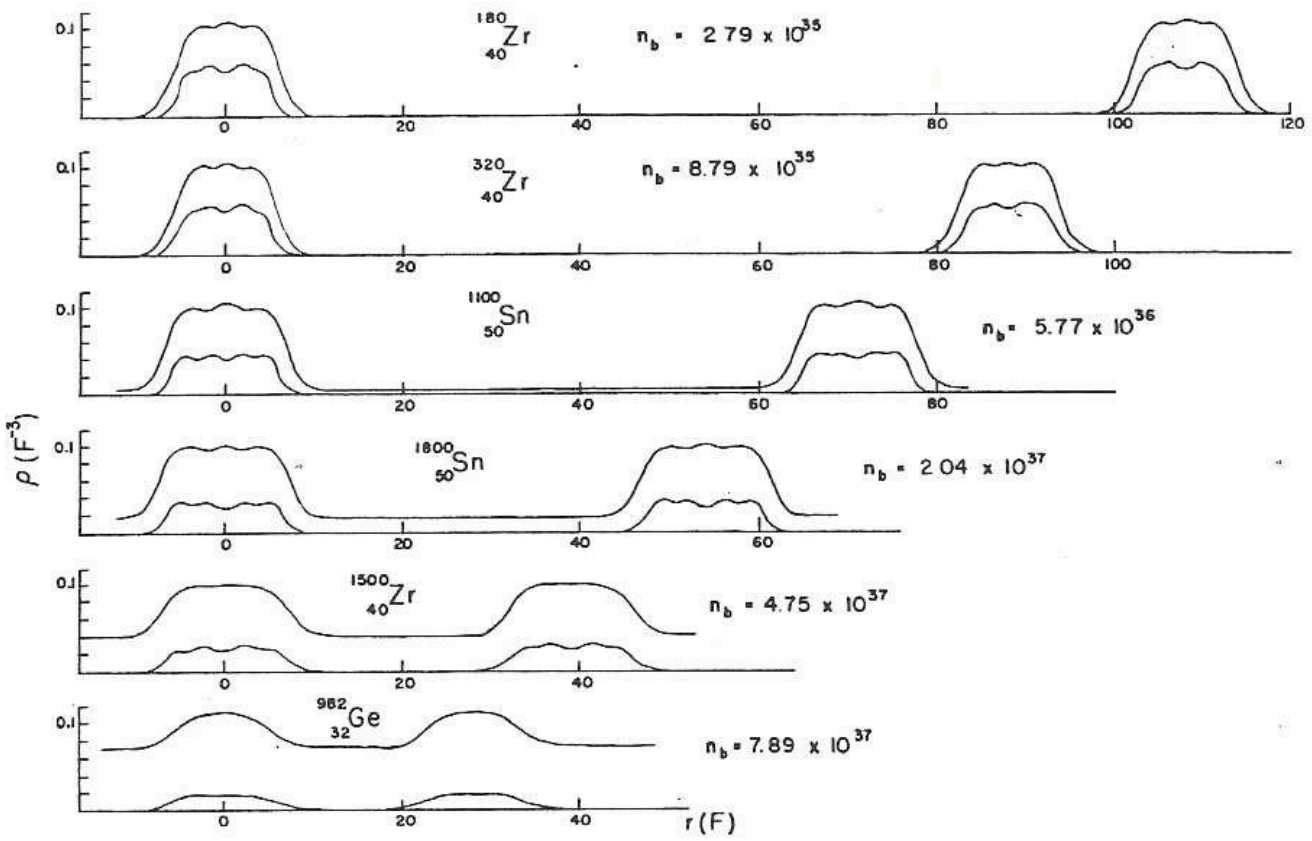

Contnuous transition from (exotic) nuclei to nuclear matter

Figure from Negele & Vautherin , NPA 207 (1973) 298

Looking for the energy minimum at a fixed baryon density

Density = 1/30 saturation density

No pairing

Wigner-Seitz approximation

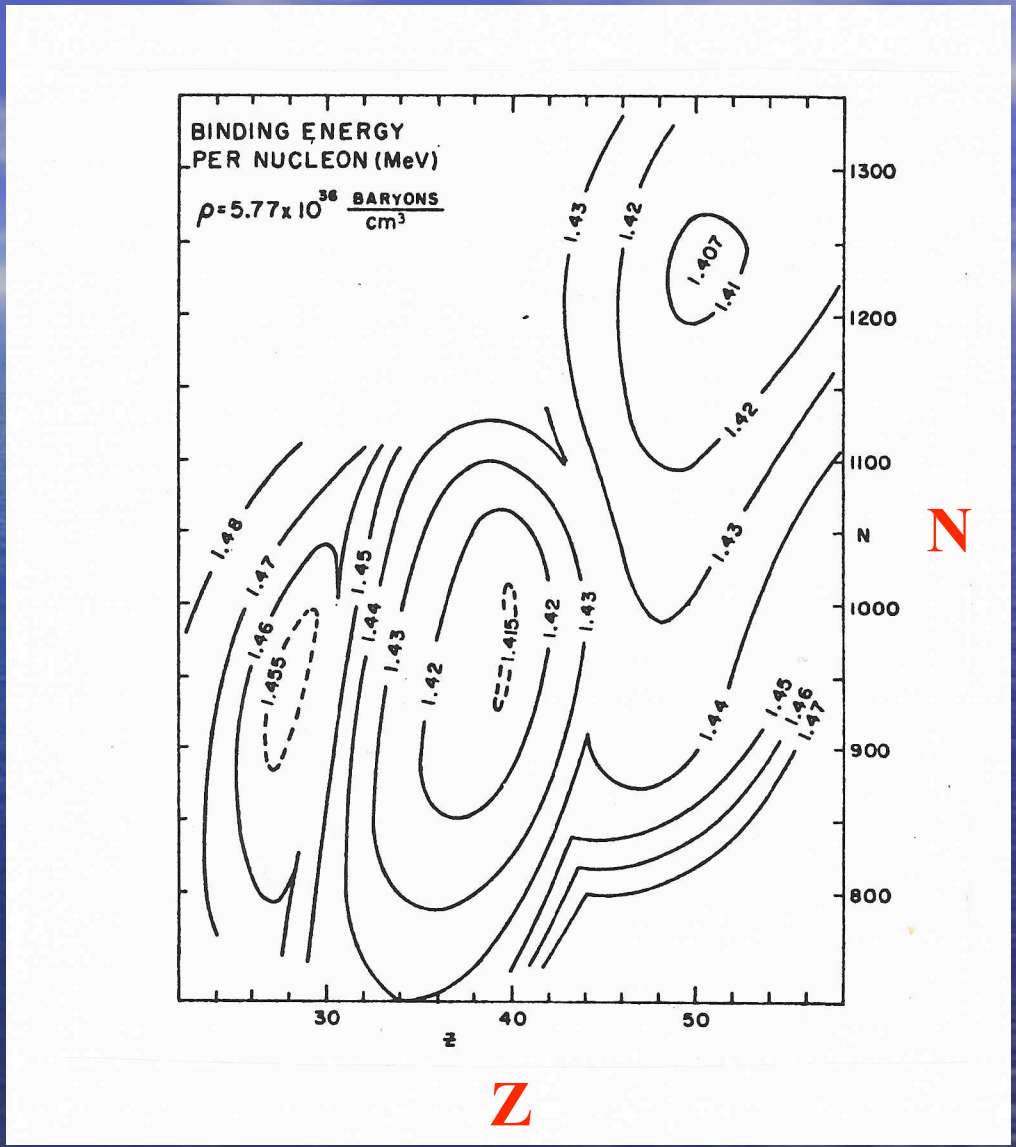

A semi-microscopic self-consistent method to describe the inner crust of a neutron star

WITHIN the Wigner-Seitz (WS) metod

With PAIRING effects included.

M. Baldo, U. Lombardo, E.E. Saperstein, S.V. Tolokonnikov,
JETP Lett. **80**, 523 (2004). –
Nuc. Phys. A **750**, 409 (2005). –
Phys. At. Nucl., **68**, 1812 (2005). –

M. Baldo, E.E. Saperstein, S.V. Tolokonnikov,
Nuc. Phys. A **775**, 235 (2006). -
Eur. Phys. J. A **32**, 97 (2007) –

M. Baldo, E.E. Saperstein, S.V. Tolokonnikov, arxiv preprint nucl-th/0703099 , PRC in press.

Developments of the method by J. Negele and D.Vautherin (NV) (1973)

1. Neutron and proton pairing.

2. Modern functional (s)

3. Study of the boundary conditions

Generally speaking the influence of pairing to the ground state configuration (Z,R_c) turned out to be strong, but the general NV pattern of the WS cell as nuclear-like clusters immersed in the sea of almost homogeneous neutrons and electrons was confirmed.

Generalized energy density functional (GEDF) method

$$E(\rho(r),\nu(r)) = E^{ph}(\rho(r),\nu(r)) \bullet F_m(r) + E^{mi}(\rho(r),\nu(r)) \bullet (1 - F_m(r))$$

$$F_m(r) = (1 + \exp((r - R_m)/d_m))^{-1},$$

$$\rho_p(R_m) = 0.1\,\rho_p(0),$$

$$d_m = 0.3\,\text{fm}.$$

Choice of F_m : outside almost homogeneous neutron matter (LDA is valid for E^{mi}), inside, where the region of big $\partial\rho/\partial r$ exists, E^{ph} dominates which KNOWS how to deal with it.

$$E(\rho,\nu) = E_{norm}(\rho) + E_{an}(\rho,\nu),$$

for phenomenological and microscopic parts.

For E^{ph} we used the DF3 functional by S.Fayans et al.

S.A. Fayans, S.V. Tolokonnikov, E.L. Trykov, and D. Zawisha, Nucl. Phys. A 6**76**, 49 (2000).
Describes a set of long isotopic chains (with odd-even effects) with high accuracy.

For E^{mi}_{norm} we used the microscopic functional by M.Baldo et al.

M.Baldo, C. Maieron, P. Schuck and X. Vinas,
Nucl. Phys. A **736**, 241 (2004).
within the Brueckner theory with the Argonne force v18 and a small addendum of 3-body forces.

Boundary conditions in WS method

$$R_{nlj}(r = R_c) = 0$$

For odd *l*, and

$$R'_{nlj}(r = R_c) = 0$$

For even *l*, boundary condition by NV (BC1),
OR *vice versa* (BC2).
Difference is essential only for larger k_F

Difference in Z value could reach 6 units –
the internal uncertainty of the WS method

We used the approach developed for the inner crust, within the WS method, to find ρ_d going from the outer crust region, $\rho \leq \rho_d$. The phenomenological (nuclear) component of GEDF should play the main role: all neutrons are bound. BUT the microscopic (neutron matter) one can not be neglected *a priori*: for bound nuclei it equivalent to a variation of the surface terms of the effective force, but they are important.

Two calculations:

1. Pure phenomenological (Fayans et al.) functional DF3,
2. Complete semi-microscopic GEDF (DF3 + Baldo et al.).

First, the pure DF3 case.

Binding energy (per a nucleon) $E_B(Z)$ for different k_F in vicinity of ρ_d by BPS (k_F=0.1977 fm^{-1}) ,
the minimum determines the g.s. (Z,R_c) at each k_F.
And $\mu_n(Z)$. Drip point: μ_n=0. k_F=0.181 fm^{-1} : ρ_d=3.30 x 10^{11} g/cm^3 (a little less than ρ_d ~4 x 10^{11} g/cm^3 by S.B. Ruster et al.) The main difference is in Z=52 (N=126) instead of Z = 34 – 38, N ~ 82 by Ruster et al. Our calculation also results in a "drip region" with Z~40, N~82, but the corresponding E_B is higher than the minimum position.

Second, the complete semi-microscopic GEDF: ρ_d =4.06 x 10^{11} g/cm^3 , k_F=0.194 fm^{-1}, but again Z=52, N=126.

Thus, the drip values, for both the cases, are shifted from Z~40, N~82 to Z~50, N~126.

i

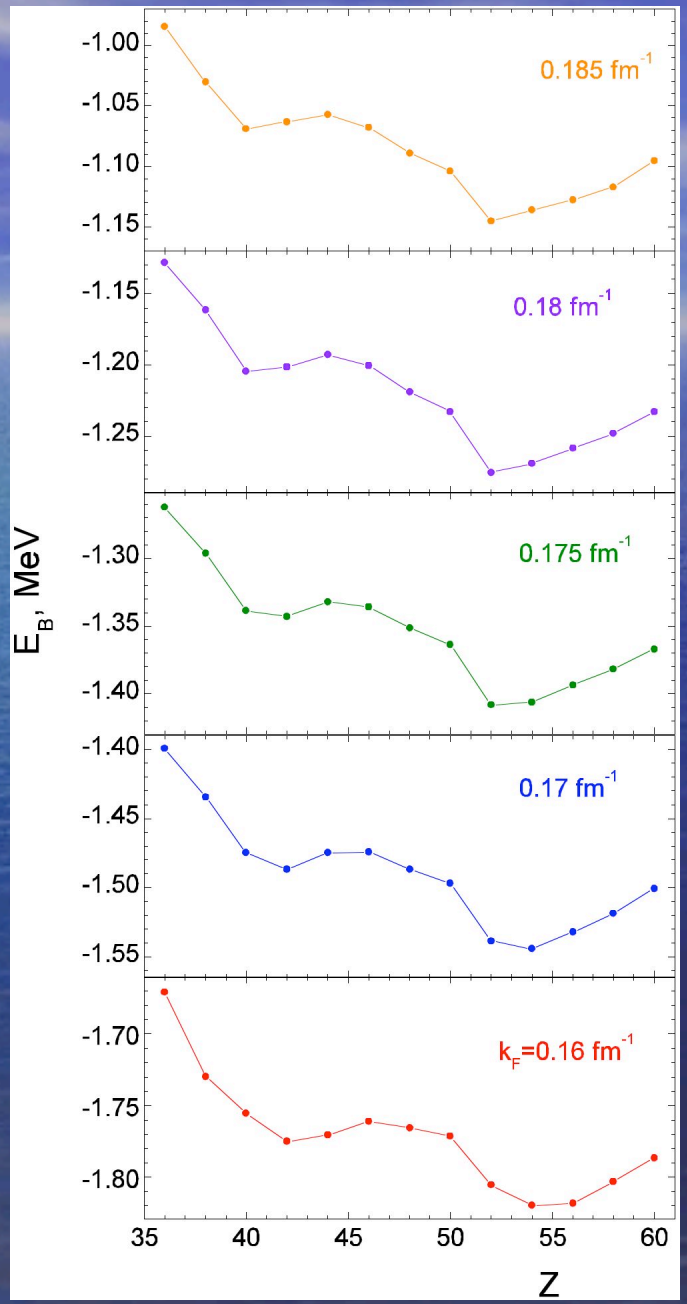
-1.00
-1.05
-1.10
-1.15
0.185 fm-1
-1.15
-1.20
-1.25
0.18 fm-1
-1.30
-1.35
-1.40
0.175 fm-1
-1.40
-1.45
-1.50
-1.55
0.17 fm-1
-1.70
-1.75
-1.80
kF=0.16 fm-1
35
40
45
50
55
60
Z
EB', MeV

μ_n for DF3 functional

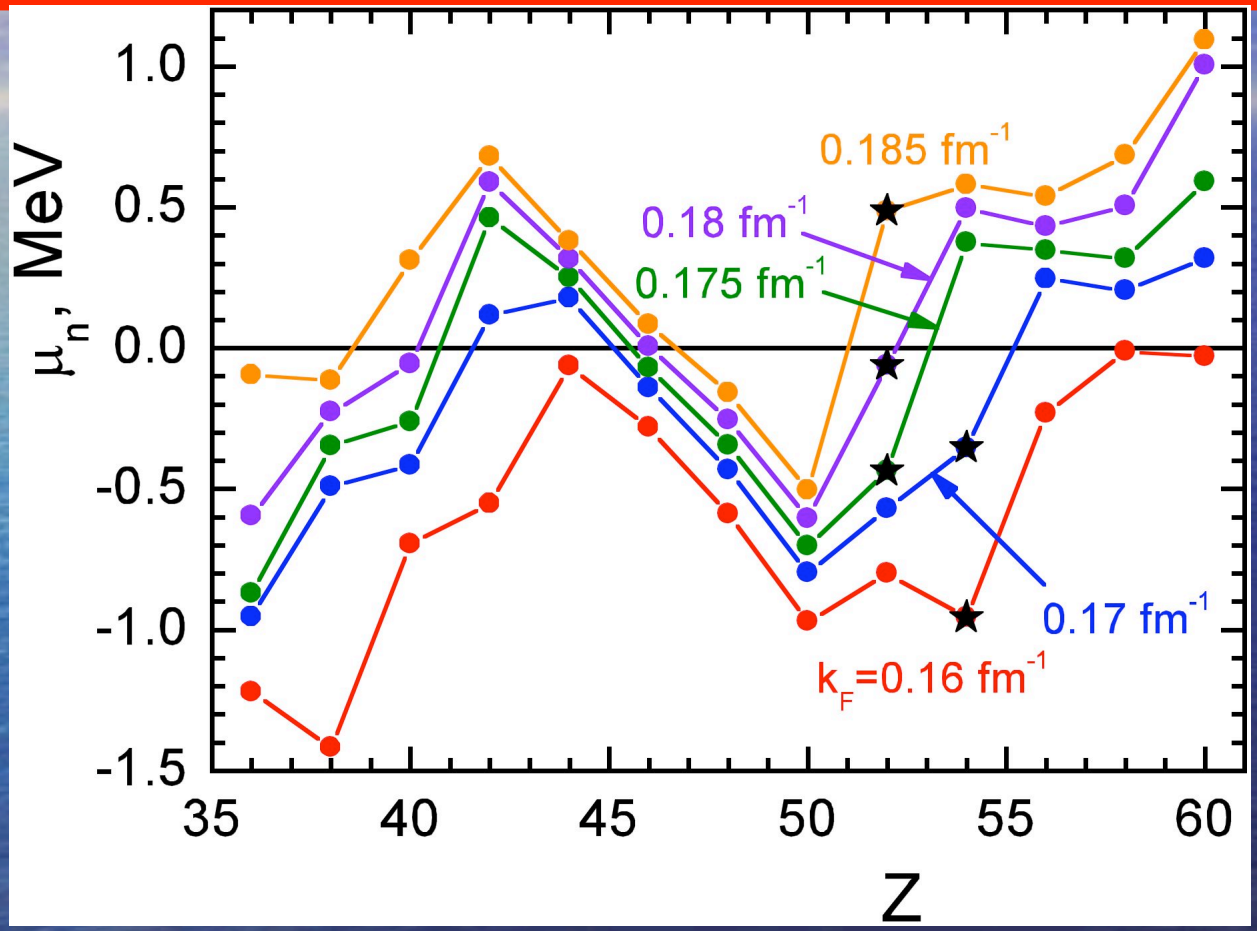

Two competing drip regions

Phenomenological DF3 functional by Fayans et al.

k_F 1/fm	Z	N	R_c Fm	E_B MeV	μ_n MeV
0.160	54	125	67.61	-1.820	-0.957
0.170	54	127	63.82	-1.544	-0.355
0.175	52	126	61.64	-1.408	-0.436
0.180	52	126	59.98	-1.275	-0.062
0.185	52	128	58.61	-1.145	0.487

Complete semi-microscopic functional

k_F 1/fm	Z	N	R_c fm	E_B MeV	μ_n MeV
0.180	52	128	60.14	-1.398	-0.868
0.190	52	126	57.85	-1.150	-0.552
0.195	52	126	57.36	-1.043	0.123
0.200	52	130	57.19	-0.950	0.194

Upper part of the inner crust

Go to densities above the drip point:

1. k_F=0.2 – 0.5 fm^{-1}
2. k_F=0.6 – 1.2 fm^{-1}

The equilibrium configuration (Z,R_c) is determined by the absolute minimum of $E_B(Z)$.

Again Z ~ 50 (NV Z=40).

Let us analyze characteristics of the central clusters in the WS cells:

$$N_{cl} = \int_{r<R_m} d^3 r \, \rho_n(r)$$

$A_{cl}=Z+N_{cl}$, R_p and R_n are defined as the points of the maximum of the gradient of ρ_p or ρ_n. (see Tabl.)

Ground state configuration (Z,R_c) is influenced by pairing effects significantly: for higher densities the Z valuee can change by a factor 2 with respect to NV .

Main reason : - β-stability condition. In fact the μ values change due to pairing much more than the total energy.

But BCS theory in neutron matter overestimates the gap significantly by a factor 2 - 3.

Eventually correlations are taken into account approximately by a suppression factor $f_{m\text{-}b}$.

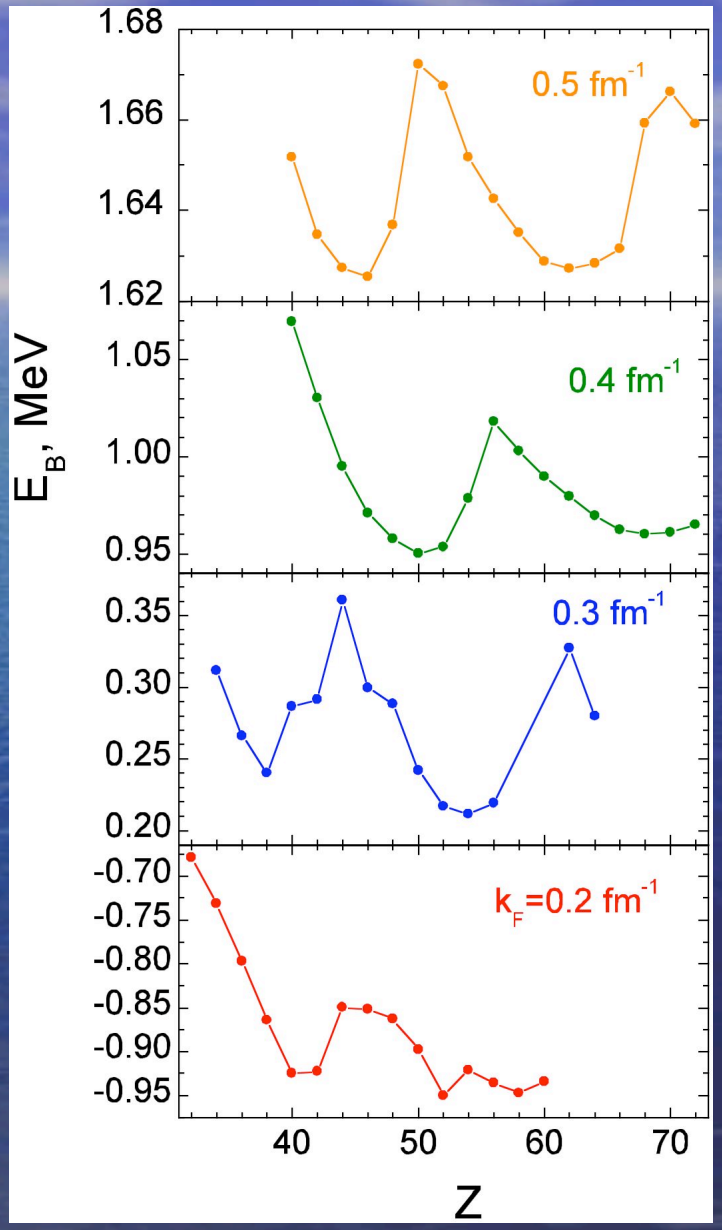
1.68
1.66
1.64
1.62
0.5 fm-1
1.05
1.00
0.95
0.4 fm-1
0.35
0.30
0.25
0.20
0.3 fm-1
-0.70
-0.75
-0.80
-0.85
-0.90
-0.95
kF=0.2 fm-1
40
50
60
70
Z
EB', MeV

Ground state characteristics of the upper parts of the inner crust

k_F, fm^{-1}	Z	A	E_B, MeV	μ_n, MeV
0.2	52	212	-0.950	0.194
0.3	54	562	0.211	1.018
0.4	50	830	0.950	1.804
0.5	46	1020	1.625	2.643

Characteristics of nuclear clusters in the upper part of the inner crust

k_F,fm^{-1}	Z	A_{cl}	R_n, fm	R_p, fm	R_c, fm
0.2	52	163	6.77	6.41	57.19
0.3	54	174	6.88	6.55	52.79
0.4	50	170	6.80	6.45	45.09
0.5	46	166	6.77	6.41	38.64

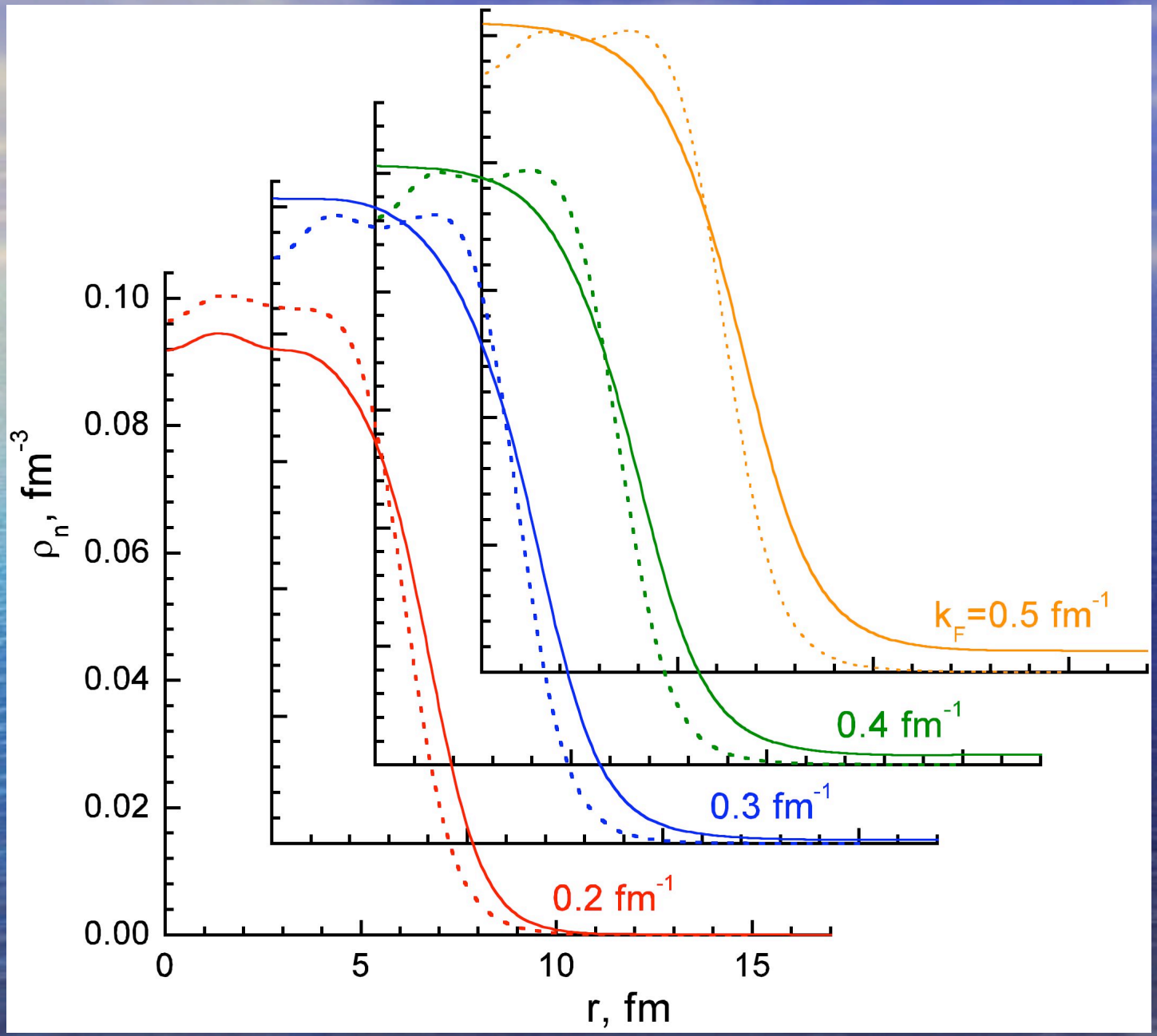
0.10
0.08
0.06
0.04
0.02
0.00
ρ_n, fm^{-3}
0
5
10
15
r, fm
k_F=0.5 fm^{-1}
0.4 fm^{-1}
0.3 fm^{-1}
0.2 fm^{-1}

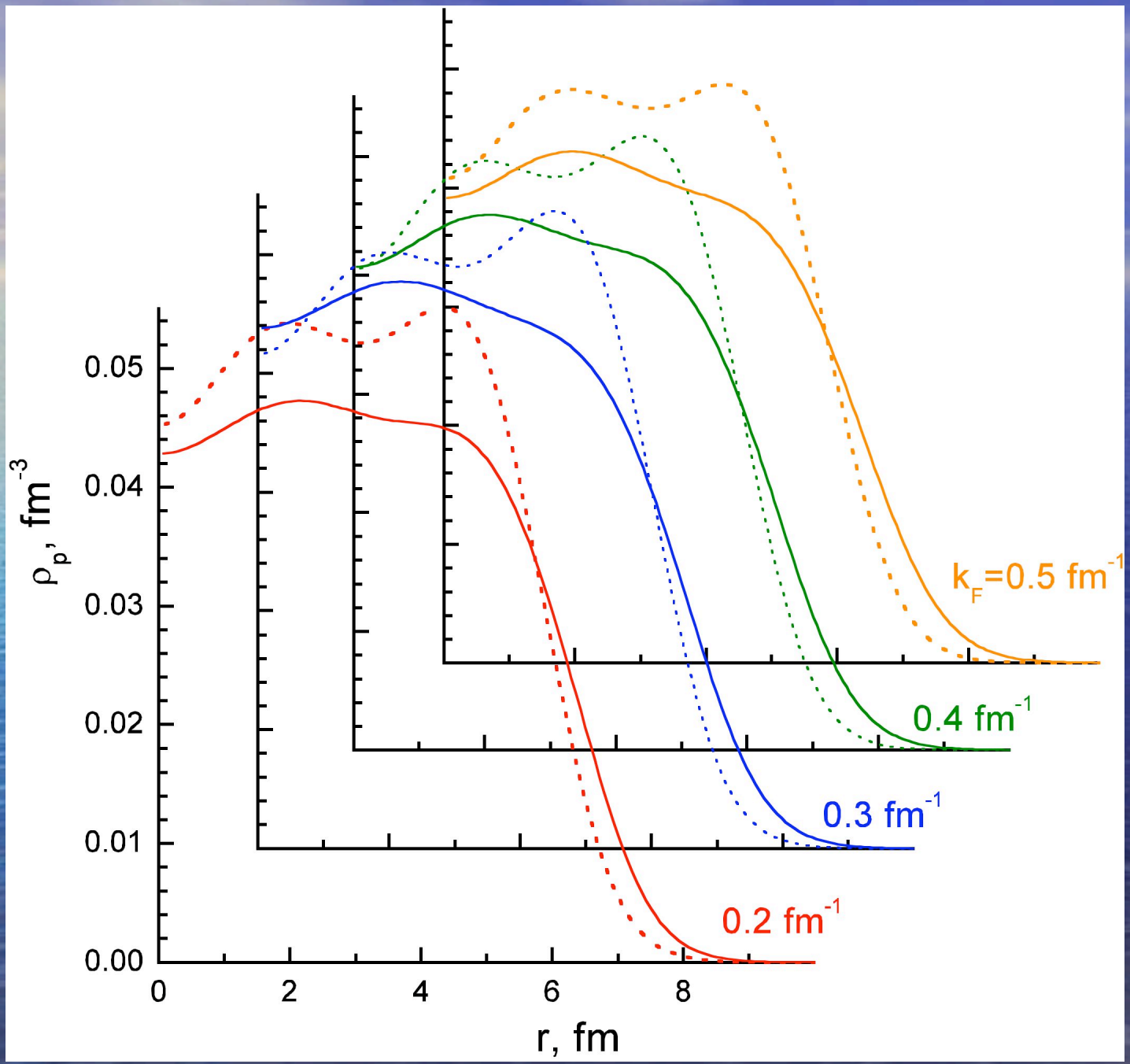
0.05
0.04
0.03
0.02
0.01
0.00
ρ_p, fm^{-3}
0
2
4
6
8
r, fm
k_F=0.5 fm^{-1}
0.4 fm^{-1}
0.3 fm^{-1}
0.2 fm^{-1}

Atomic nuclei with such (Z,A_{cl}) are still stable for the strong interaction:

Comparing density distributions for clusters and nuclear counterparts (Figs.), they look quite close to each other, radii and diffuseness parameters for clusters are bigger, but only slightly.

Consider $\Delta_n(r)$ (Fig.) : Direct solution of the gap equation versus LDA calculation. In the asymptotic region, the difference is ~10–15%.

Inside the cluster, nothing in common. Strong "proximity" effect in the direct solution: inside-outside interplay - $\Delta_n(0) \approx \Delta_n(r \sim R_c)$, contrary to LDA.

$\Delta_n(r)$: direct solution versus LDA

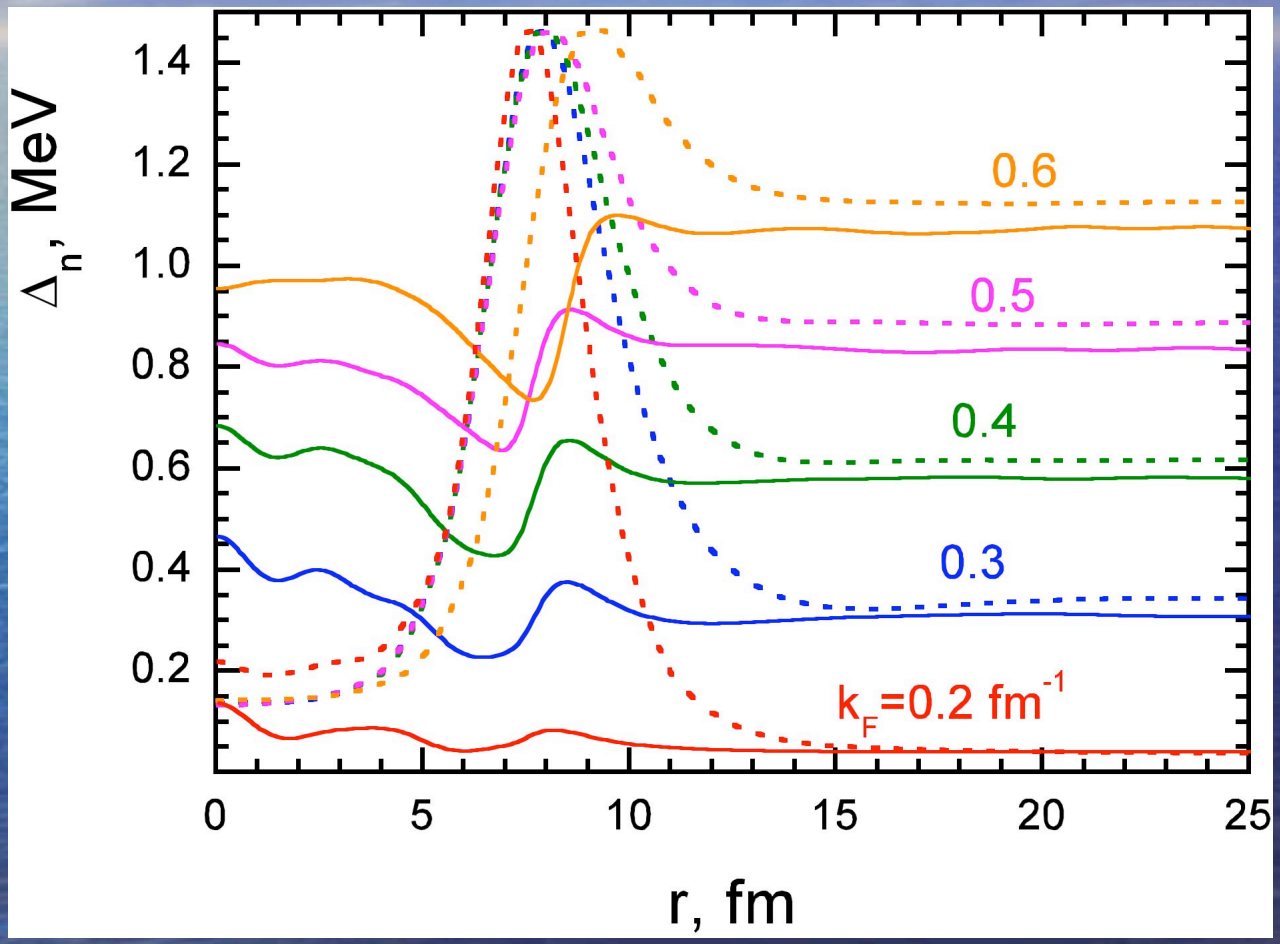

Pairing gap suppressed by a factor 2

Results for the upper part of the inner crust

Main new feature of our calculations is the shift of the equilibrium Z values.

In the density region under consideration, from Z~40 to Z~50.

The results depend not only on pairing effects, but also on the peculiarities of the semi-microscopic GEDF used

For the drip point vicinity the phenomenological DF3 component is more important.

Density = 1/10 saturation density , Wigner-Seitz cell

Neutron and proton density profiles

Neutron and proton pairing profiles

NPA 775 (2006) 235
M.B., E.E. Saperstein
S.V. Tolokonnikov.

Functional compatible with microscopic nuclear matter calculations

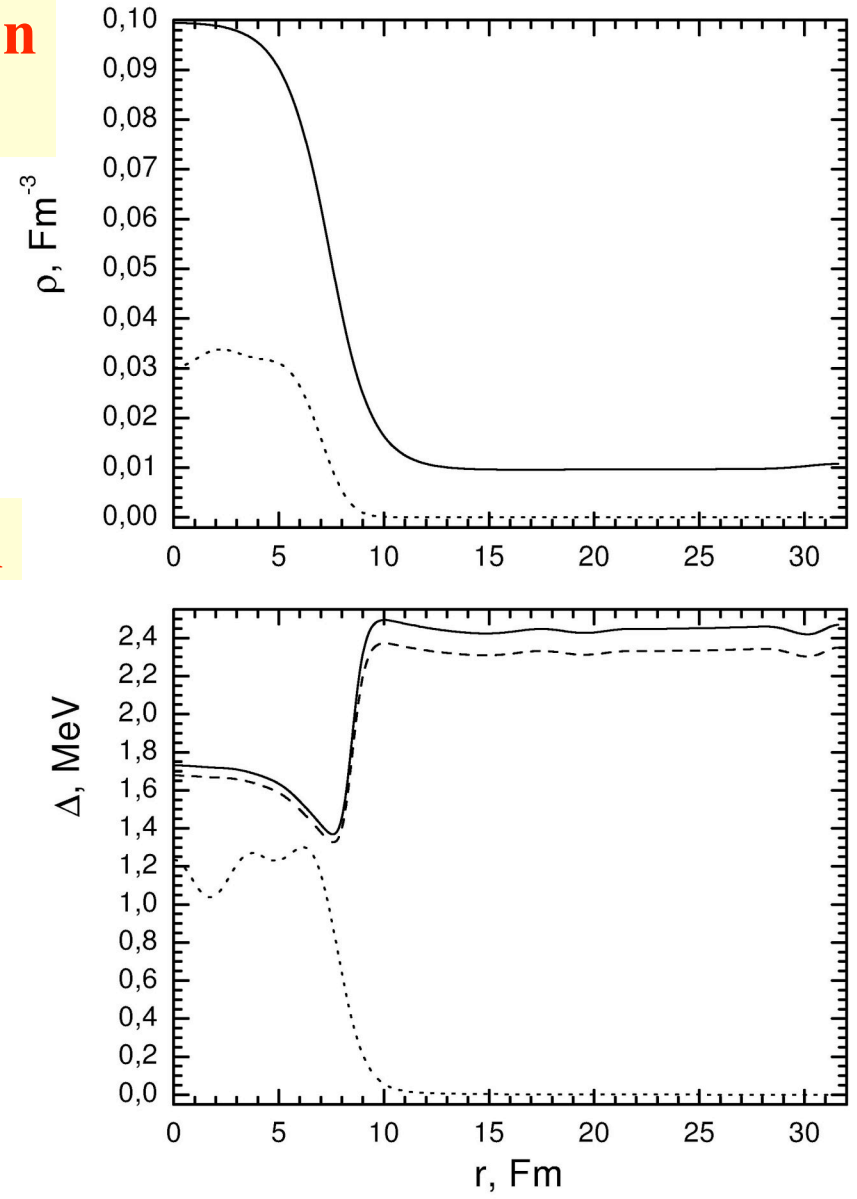

In search of the energy minimum as a function of the Z value inside the WS cell

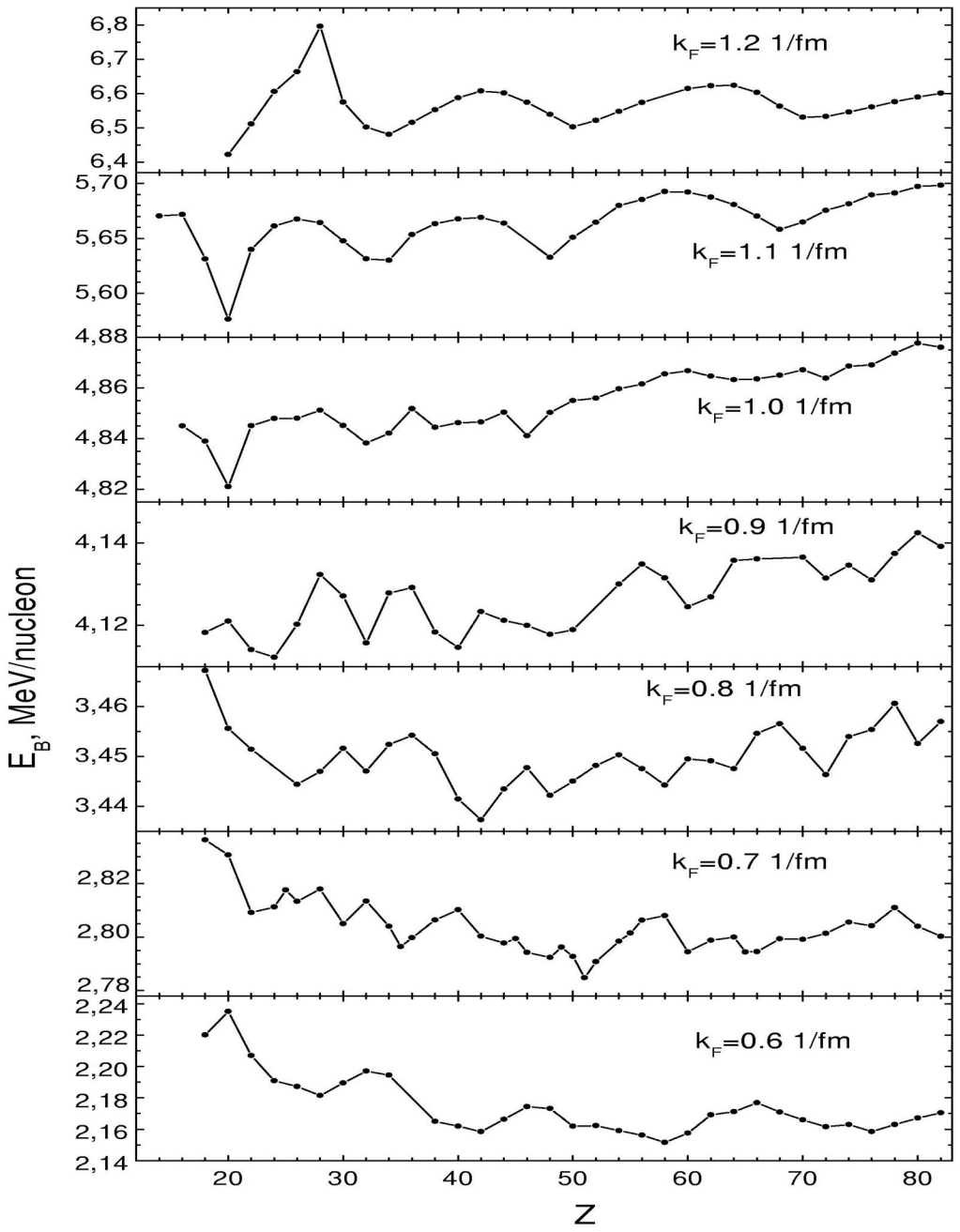

Dependence on the boundary conditions at different densities

Only at the higher densities the boundary conditions matter

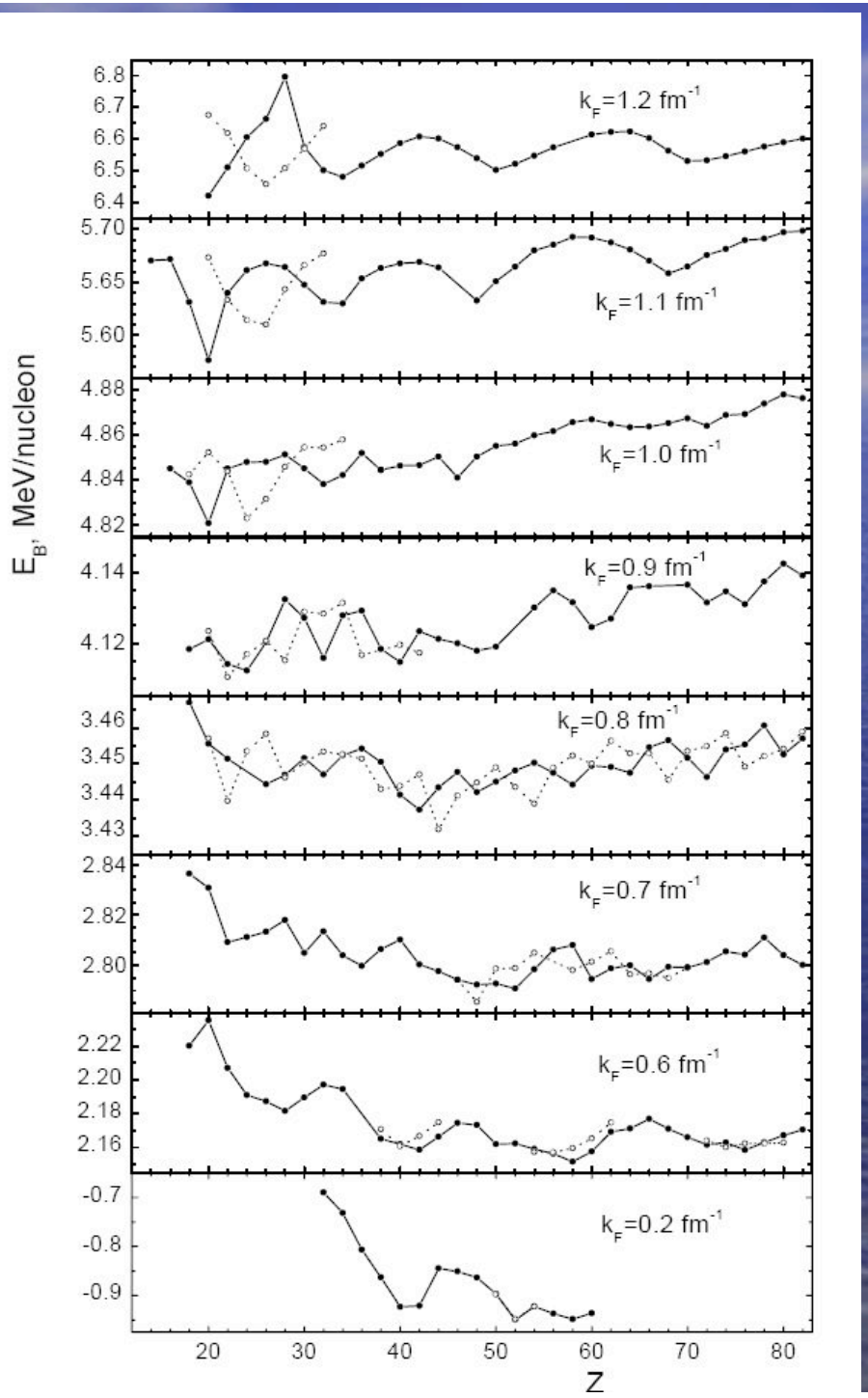

Characteristics of the ground state configurations of the WS cell at various densities.

k_F, fm^{-1}	Z	Z 1	A	R_c, fm	x	x 1	x 2
0.6	58	50	1612.10	37.505	0.036	0.037	0.0004
0.7	51	50	1573.70	31.890	0.032	0.037	0.0010
0.8	42	50	1409.10	26.895	0.030	0.028	0.0019
0.9	24	50	857.02	20.255	0.028	0.028	0.0034
1.0	20	40	658.07	16.693	0.030	0.027	0.0057
1.1	20	40	634.62	14.993	0.032	0.027	0.0086
1.2	20	40	626.47	13.684	0.032	0.027	0.0125

1 Negele & Vautherin

2 Uniform nuclear matter (M.B.,Maieron,Schuck,Vinas NPA 736, 241 (2004))

EOS of the crust

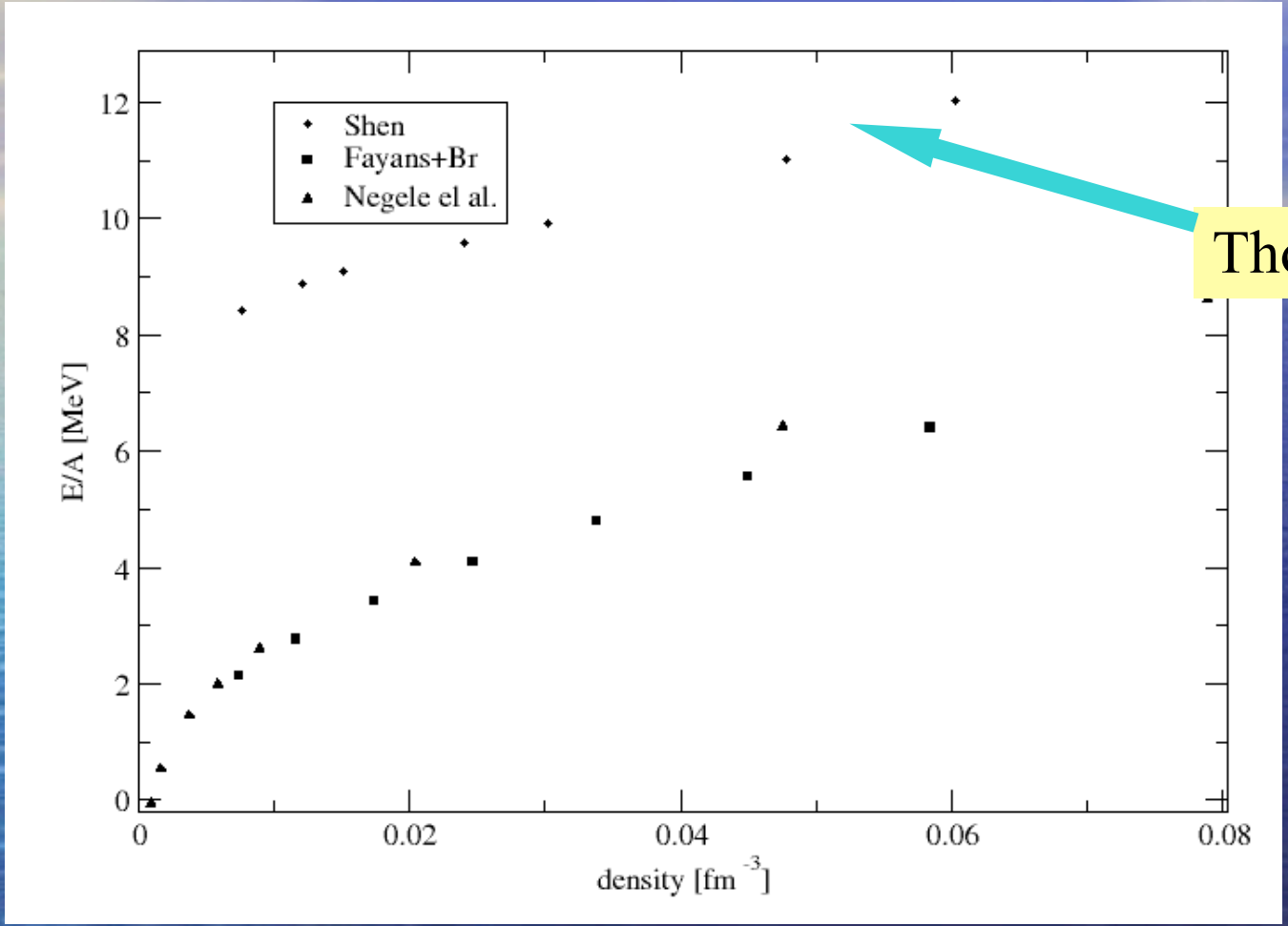

Thomas-Fermi

Comparing different Equations of State for low density

Reducing the pairing gap

$\Delta = \Delta_{BCS}$

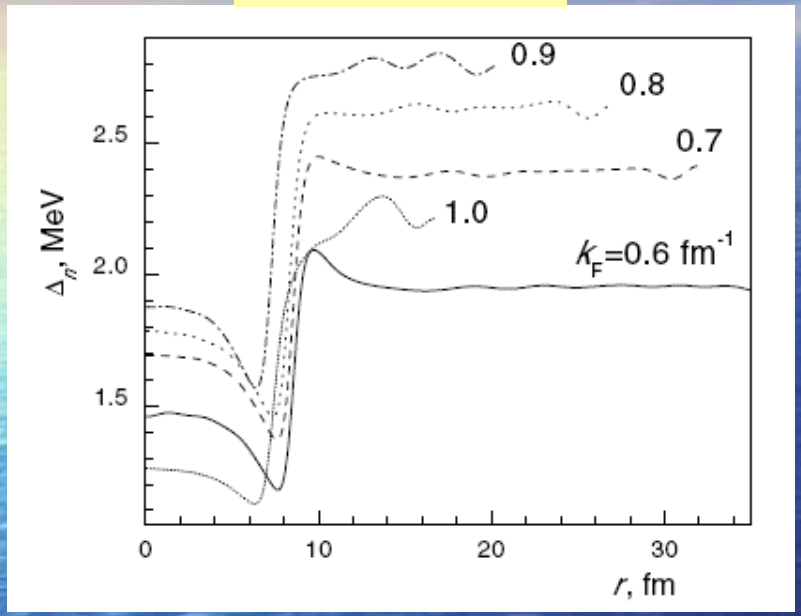

$\Delta = \Delta_{BCS} / 2$

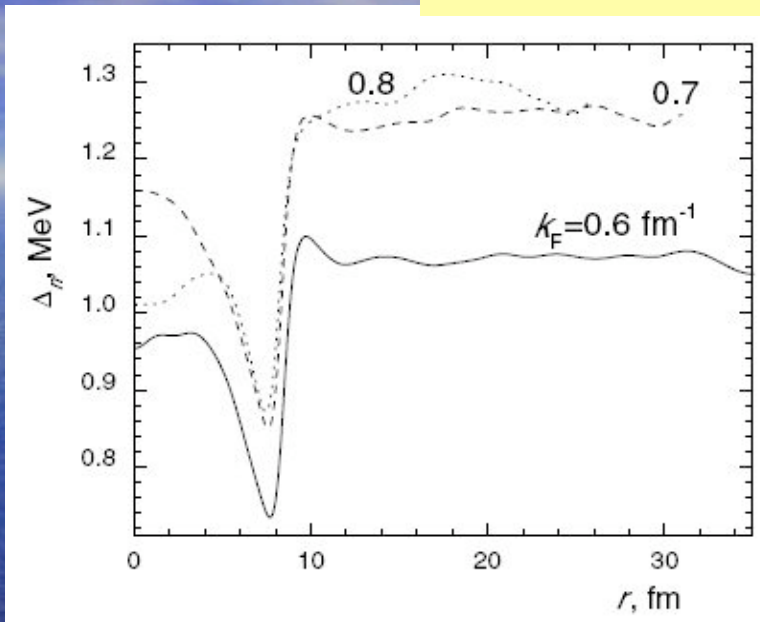

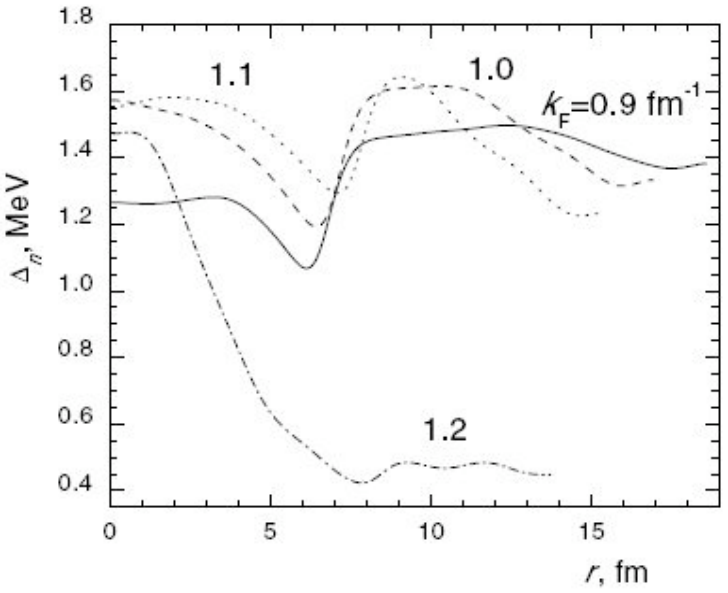

$$\Delta = \Delta_{BCS}$$

k_F, fm^{-1}	Z	k_F^{as}, fm^{-1}		$\Delta(0)$, MeV		Δ_{as}, MeV		Δ_F, MeV		Δ_{inf}, MeV		Δ^0_{inf}, MeV
		BC1	BC2	BC1	BC2	BC1	BC2	BC1	BC2	BC1	BC2	
0.2	52	0.1156	0.1095	0.088	0.132	0.042	0.046	0.043	0.058	0.126	0.106	0.40
0.6	58	0.5786	0.5783	1.464	1.471	1.947	1.899	1.919	1.893	2.321	2.320	2.42
	56	0.5783	0.5786	1.456	1.428	1.899	1.912	1.893	1.891	2.319	2.321	
0.7	52	0.6758	0.6753	1.665	1.650	2.358	2.288	2.300	2.247	2.680	2.678	2.76
	48	0.6763	0.6763	1.679	1.648	2.312	2.368	2.290	2.325	2.682	2.682	
0.8	42	0.7732	0.7724	1.767	1.726	2.614	2.546	2.555	2.445	2.883	2.882	2.93
	44	0.7729	0.7727	1.747	1.834	2.580	2.679	2.525	2.560	2.883	2.883	
0.9	24	0.8694	0.8693	1.862	1.664	2.777	2.625	2.636	2.506	2.919	2.919	2.92
	22	0.8725	0.8664	1.936	1.654	2.677	2.680	2.617	2.544	2.918	2.919	
1.0	20	0.9499	0.9613	1.249	1.966	2.199	2.635	2.023	2.517	2.800	2.773	2.68
	24	0.9612	0.9574	1.894	1.504	2.705	2.507	2.519	2.288	2.774	2.782	
1.1	20	1.0315	1.0531	0.996	1.889	1.477	2.411	1.318	2.317	2.550	2.458	2.26
	26	1.0434	1.0649	1.927	1.296	2.469	2.242	2.280	2.020	2.500	2.408	
1.2	20	1.1243	1.1321	1.556	0.992	1.340	2.017	1.210	1.558	2.113	2.066	1.66
	26	1.1278	1.1160	0.760	0.991	1.549	0.963	1.249	0.862	2.092	2.163	

$\Delta(0)$ Gap at the center of the WS cell

Δ_{as} Gap at large distance

Δ_F Gap at the Fermi energy

Δ_{inf} Gap corresponding to the asymptotic density

$$\Delta = \Delta_{BCS} / 2$$

k_F, fm^{-1}	Z	k_F^{as}, fm^{-1}		$\Delta(0)$, MeV		Δ_{as}, MeV		Δ_F, MeV		Δ_{inf}, MeV		Δ_{inf}^0, MeV
		BC1	BC2	BC1	BC2	BC1	BC2	BC1	BC2	BC1	BC2	
0.6	56	0.5797	0.5790	0.971	0.962	1.058	1.056	1.059	1.051	1.163	1.161	1.21
	54	0.5783	0.5781	0.980	0.946	1.063	1.042	1.050	1.048	1.160	1.159	
0.7	46	0.6760	0.6760	1.057	1.104	1.241	1.244	1.211	1.244	1.340	1.341	1.38
	48	0.6784	0.6750	1.141	1.044	1.248	1.202	1.235	1.213	1.345	1.339	
0.8	40	0.7691	0.7752	1.025	1.231	1.264	1.360	1.256	1.346	1.438	1.443	1.46
0.9	20	0.8514	0.8769	0.608	1.271	0.834	1.374	0.816	1.401	1.460	1.459	1.46
	26	0.8670	0.8820	1.113	1.325	1.305	1.323	1.320	1.320	1.459	1.459	
1.0	20	0.9399	0.9675	0.024	1.523	0.041	1.329	0.037	1.453	1.411	1.380	1.34
	24	0.9630	0.9344	1.465	0.447	1.339	0.644	1.426	0.621	1.385	1.418	
1.1	20	1.0315	1.0580	0.015	1.576	0.026	1.245	0.022	1.424	1.275	1.219	1.13
	24	1.0549	1.0258	1.439	0.804	1.253	0.649	1.393	0.658	1.226	1.287	
1.2	20	1.1253	–	1.229	–	0.461	–	0.539	–	1.053	–	0.83
	26	1.1306	1.1146	0.177	0.050	0.305	0.068	0.309	0.061	1.037	1.086	

$$\Delta = \Delta_{BCS} / 3$$

k_F, fm^{-1}	Z	k_F^{as}, fm^{-1}		$\Delta(0)$, MeV		Δ_{as}, MeV		Δ_F, MeV		Δ_{inf}, MeV		Δ^0_{inf}, MeV
		BC1	BC2	BC1	BC2	BC1	BC2	BC1	BC2	BC1	BC2	
0.6	56	0.5817	0.5788	0.721	0.755	0.719	0.713	0.723	0.715	0.778	0.774	0.81
	54	0.5787	0.5792	0.755	0.701	0.732	0.704	0.722	0.713	0.774	0.775	
0.7	46	0.6752	0.6782	0.789	0.850	0.832	0.852	0.806	0.865	0.893	0.896	0.92
	48	0.6826	0.6739	0.924	0.765	0.864	0.797	0.864	0.817	0.901	0.891	
0.8	40	0.7676	0.7791	0.699	1.019	0.787	0.923	0.799	0.943	0.958	0.964	0.91
0.9	20	0.8489	0.8828	0.080	1.019	0.107	0.887	0.097	0.975	0.974	0.972	0.90
	24	0.8747	0.8450	0.995	0.367	0.817	0.468	0.919	0.479	0.973	0.974	
1.0	20	0.9399	0.9690	0.011	1.335	0.019	0.919	0.017	1.100	0.941	0.919	0.89
	24	0.9636	0.9323	1.291	0.134	0.909	0.167	1.068	0.174	0.923	0.947	
1.1	20	1.0315	1.060	0.035	1.472	0.028	0.907	0.028	1.154	0.850	0.810	0.75
	24	1.0583	1.0261	1.236	0.618	0.899	0.375	1.10	0.419	0.812	0.858	
1.2	20	1.1254	1.1458	1.154	0.010	0.313	0.013	0.418	0.018	0.702	0.661	0.55
	26	1.1308	1.1146	0.157	0.111	0.239	0.021	0.270	0.031	0.691	0.724	

OUTLOOK

1. Different accurate functionals for the structure.
   This appears the main uncertainity
   (symmetry energy ?)

2. The EOS seems to be less sensitive (Oscillations,….)

3. Excitations/Finite temperature

4. Include deformations

4. Structure from band theory (Meudon group)

5. Inter-band Cooper pairs